processes

MDPI

Article

Simulation of Hydrogen-Blended Natural Gas Leakage in Confined Space

Nuo Xu [1,2], Zhiyu Yang [3,*], Qianqian Shao [1], Lin Wang [1] and Ruijiang Yu [1]

1 School of Petroleum Engineering, Guangdong University of Petrochemical Technology, Maoming 525000, China; yqcy2026@163.com (L.W.)
2 School of Petroleum Engineering, Northeast Petroleum University, Daqing 163000, China
3 College of Pipeline and Civil Engineering, China University of Petroleum (East China), Qingdao 266580, China
* Correspondence: z25060066@s.upc.edu.cn

Abstract

As a key enabler for carbon neutrality, hydrogen-blended natural gas utilization requires a thorough safety assessment. This study investigates leakage dispersion in a typical kitchen (4 m × 3 m × 2.8 m) using validated CFD methods. Simulations examined coupled effects of hydrogen blending ratios (0–20%), leakage types (pipe cracks/hose pinholes), and ventilation conditions. Results show hydrogen enrichment accelerates overall dispersion but intensifies methane accumulation near the source. In all scenarios, buoyancy-driven stratification formed stable combustible layers (>0.3 m thick) exceeding the mixture-specific lower flammability limit (recalculated using Le Chatelier's law) after 25 min in confined spaces. While ventilation promoted global diffusion, it created persistent high-concentration zones (≥5% volume fraction) near leakage sources. The spatial overlap of these hazardous clouds with ignition sources significantly increases explosion risks. This research provides critical insights for developing safety standards and emergency protocols for hydrogen–natural gas mixtures.

Keywords: hydrogen-blended natural gas (HNG); confined space; leakage and dispersion; computational fluid dynamics; turbulence model; explosion risk

1. Introduction

Hydrogen energy has emerged as a strategic focus in the global low-carbon transition of energy structures due to its advantages of high calorific value, zero carbon emissions, and diversified production pathways. However, the large-scale storage and transportation of hydrogen face dual challenges in terms of safety and economics: its physical properties such as low density, wide flammability range, and high permeability impose stricter requirements on transmission and distribution systems, while the substantial investment required for new pure-hydrogen pipeline networks severely restricts the rapid development of the hydrogen energy industry. How to achieve efficient and safe utilization of hydrogen has increasingly become a core issue of academic concern [1,2]. Current research generally agrees that utilizing existing natural gas pipeline systems to transport hydrogen in the form of hydrogen-blended natural gas is one of the most important pathways for achieving large-scale economical hydrogen transportation [3–6].

Lynch et al. [7] were among the first to propose the technical concept of using existing natural gas pipelines to transport hydrogen blended with natural gas at specific ratios, aiming to provide a feasible solution for deep decarbonization in industrial and building

Academic Editor: Zhenmin Cheng

Received: 12 April 2026
Revised: 2 June 2026
Accepted: 3 June 2026
Published: 8 June 2026

sectors. Over recent decades, countries including those in Europe, America, and China have conducted extensive research, focusing on the impacts of key parameters such as hydrogen blending ratio, stratification of hydrogen-blended natural gas, and material compatibility on system safety and end-use applicability. Several landmark demonstration projects for hydrogen-blended natural gas have been successively commissioned [8], advancing this technology from conceptual validation to initial engineering practice.

To facilitate the safe and efficient integration of hydrogen energy into end-use energy consumption, it is imperative to systematically address the technical bottlenecks of hydrogen-blended natural gas across the entire industry chain. Among these, the end-user segment, as the final link in realizing the "hydrogen to every household" strategy, is particularly critical for safety assurance—especially in confined spaces commonly associated with urban gas use, such as residential kitchens and boiler rooms in northern winter heating systems. Statistics indicate that the severity and casualty rates of gas leakage accidents in confined spaces are significantly higher than those in open environments. Therefore, ensuring the safe utilization of hydrogen energy must prioritize understanding the leakage and dispersion mechanisms and risk prevention and control technologies in such scenarios.

This paper addresses the leakage of hydrogen-blended natural gas in partially confined spaces with openings, systematically investigating the influence of ventilation conditions on the quasi-steady-state dispersion behavior of leaked gas. The research findings will provide theoretical support for the large-scale engineering application of hydrogen-blended natural gas and offer a scientific basis for revising urban gas safety management regulations.

Current research on the leakage behavior of hydrogen-blended natural gas primarily relies on physical experimental methods, which inherently suffer from limitations such as high costs, operational safety risks, and poor flexibility in reproducing working conditions. Consequently, computational fluid dynamics (CFD) numerical simulation technology, leveraging its advantages in modeling complex scenarios and analyzing multi-parameter coupling, has become an efficient alternative for studying the leakage-dispersion mechanisms of hydrogen-blended natural gas and has gained widespread application in this field.

In the 1980s, Lawrence Livermore National Laboratory in the United States pioneered the development of the FEM3 computational model [9], based on the finite element discretization method and a one-equation k-turbulence model, successfully reproducing the dispersion behavior in the Thorney Island large-scale transient leakage experiments. After iterative upgrades, this model evolved into the two-way coupled turbulence model FEM3C [10], significantly improving the simulation accuracy of turbulent transport under complex boundary conditions.

In the study of leakage mechanisms of hydrogen-blended natural gas, POLMAN et al. [11] revealed the migration characteristics of hydrogen-blended natural gas by monitoring the evolution of hydrogen volume fraction in a confined space: under the same leakage pressure, hydrogen blending significantly increases the jet velocity of the mixed gas; when the hydrogen volume fraction exceeds 0.7, obvious stratification occurs in the initial leakage phase due to density differences. Wilkening [12], using the CFD-ACE platform, compared the pipeline leakage behaviors of natural gas and pure hydrogen, finding that hydrogen's higher molecular diffusion coefficient and lower density lead to a faster leakage rate, but the dispersion range of its lower flammability limit (LFL) is significantly smaller than that of natural gas, indicating that hydrogen's local combustion and explosion risk in open spaces is relatively controllable.

In the study of leakage and dispersion characteristics of hydrogen-blended natural gas pipelines, Wang Xin et al. [13] established a numerical leakage model under obstructed conditions based on fluid dynamics theory. Simulation analysis revealed that as the hydrogen blending ratio increases, the horizontal and vertical dispersion ranges of hydrogen expand significantly, while the dispersion range of methane correspondingly decreases. Furthermore, SU et al. [14] conducted numerical simulation studies on the leakage behavior of hydrogen-blended natural gas in kitchen environments. The results showed that under constant leakage rate conditions, an increase in the hydrogen blending ratio significantly shortens the time for the gas to reach the response threshold of combustible gas alarms after leakage, while also advancing the time for the mixture to reach the lower flammability limit (LFL). These studies collectively highlight the significant influence of the hydrogen blending ratio on the dispersion behavior and safety characteristics of leaked gas, providing a theoretical basis for risk prevention and control of hydrogen-blended natural gas.

Wang Jianping et al. [15] used Fluent software to develop numerical models for three typical leakage modes: crack leakage, pinhole leakage, and complete pipeline rupture. This research systematically analyzed the dynamic evolution of combustible gas clouds post-leakage and the influencing mechanisms of relevant factors, supplemented by small-scale similarity experiments for validation. The results demonstrated that numerical simulations based on standard algorithms can accurately reflect the leakage and dispersion characteristics of natural gas in kitchen environments. However, research on high-pressure hydrogen and hydrogen-blended natural gas leakage is often constrained by time, space, economic, and safety feasibility, leading to certain deviations between existing research results and actual situations. Specifically, current studies exhibit the following shortcomings: First, there is a lack of systematic and detailed explanation of the numerical simulation and solution processes for natural gas leakage under different hydrogen blending ratios; second, insufficient comparison of leakage and dispersion differences under various ventilation conditions, such as closed (e.g., windows shut) and semi-confined (e.g., windows open) scenarios in actual confined spaces; finally, there remains a lack of sufficient, multi-faceted empirical data to support the objective accuracy of numerical simulation results.

To systematically investigate the leakage and dispersion patterns of hydrogen-blended natural gas in confined spaces, this study establishes a full-scale physical model measuring 4 m × 3 m × 2.8 m. Based on statistical analyses of domestic and international gas accidents, two most representative leakage types (e.g., sustained leakage through a small orifice and instantaneous large-flow leakage) are selected to systematically simulate the leakage behavior of natural gas with different hydrogen blending ratios (e.g., 0–20% vol).the

Numerically, the study employs the shear stress transport (SST k-ω) turbulence model based on the Reynolds-averaged Navier–Stokes equations. This model offers high accuracy in predicting near-wall flows and separated flows, enabling precise capture of the spatiotemporal evolution of combustible gas clouds. By coupling with a species transport model and utilizing CFD-POST for efficient post-processing, quantitative data on the volume fraction distributions of hydrogen and methane at key locations within the confined space (e.g., near the leakage source, ceiling accumulation area, door and window openings) are obtained, along with the time and spatial range for the combustible cloud volume fraction to reach the lower flammability limit (LFL).

Novelty and contribution of this study: Compared with previous CFD studies on hydrogen-blended natural gas (HNG) kitchen leakage, particularly Su et al. [14] (Renewable Energy, 2022) which focused primarily on the effects of hydrogen blending ratio, leak rate, and room size, the present work provides three distinctive contributions. First, it systematically compares two physically different leakage forms (crack leakage vs. pinhole leakage) that represent chronic degradation and acute penetration failure modes, respectively. Second, it quantifies the coupled effects of hydrogen blending ratio, leakage type, and ventilation condition (confined vs. open window) on gas migration pathways, vertical stratification characteristics, and the transient formation process of flammable clouds. Third, it evaluates the spatial overlap between hazardous zones and potential ignition sources (e.g., stove and ceiling light), providing engineering-relevant insights for alarm placement and emergency response. These aspects have not been systematically addressed in previous HBNG indoor leakage studies.

The core objective of this study is, through the aforementioned numerical simulations, to systematically compare the effects of hydrogen blending ratio on gas dispersion paths, vertical stratification characteristics, volume fraction decay patterns, and the formation speed of combustible regions under two typical practical scenarios: closed (doors and windows shut) and semi-confined (partially open window). This aims to establish a more engineering-relevant predictive methodology for the leakage and dispersion of hydrogen-blended natural gas, ultimately providing solid theoretical support and quantitative basis for safety regulations, leakage monitoring and alarm placement, and emergency response planning in residential and commercial indoor environments using hydrogen-blended natural gas.

2. Mathematical Model

The dispersion process of hydrogen-blended natural gas after leakage in a confined space involves complex turbulent flow characterized by multicomponent, compressible, and unsteady features. To fully describe this physical process, this study establishes a closed set of governing equations, including mass conservation (continuity equation), momentum conservation (Navier–Stokes equations), energy conservation (energy equation), turbulent transport, and species transport equations.

Given that the leakage jet and subsequent spatial dispersion involve significant turbulent effects, particularly near-wall flows and potential flow separation, this study adopts the widely validated shear stress transport (SST) k-ω model for engineering turbulence simulations. This model skillfully combines the robustness of the k-ω model in near-wall computations with the superiority of the k-ε model in far-field regions, enabling more accurate prediction of turbulent shear stresses under complex flow conditions. Consequently, it facilitates the numerical simulation of the spatiotemporal evolution laws of combustible gas clouds formed after the leakage of hydrogen-blended natural gas.

(1) Gas Continuity Equation

$$\frac{\partial \rho}{\partial t} + \nabla \cdot (\rho u) = 0 \tag{1}$$

where

ρ—the density of the hydrogen-blended natural gas mixture, kg/m^3;
t—the time, s;
u—is the velocity vector, m/s.

(2) Momentum Conservation Equation

$$\frac{\partial (\rho u)}{\partial t} + \nabla \cdot (\rho u u) = -\nabla \cdot p + \nabla \cdot \tau_{eff} + \rho g \tag{2}$$

Note: The term $\nabla \cdot (\rho u u)$ represents the convective momentum flux term; no factor of 1/2 is present, consistent with the standard momentum conservation equation.

u—the velocity vector, m/s;
p—the pressure, Pa;
τ_{eff}—the effective stress tensor, Pa;
g—the gravitational acceleration vector, m/s^2.

(3) Gas Energy Conservation Equation:

$$\frac{\partial (\rho E)}{\partial t} + \nabla \cdot [u(\rho E + p)] = \nabla \cdot \left(K_{eff} \nabla \cdot T - \sum_j H_j J_j + \tau_{eff} u \right) \tag{3}$$

where:

E—total energy per unit mass of the gas mixture, J/kg;
K_{eff}—effective thermal conductivity, W/(m·K);
T—temperature, K;
H_j—specific enthalpy of species j, J/kg;
J_j—diffusion flux of species j, kg/(m^2·s);
j—number of species in the hydrogen-blended natural gas mixture.

(4) Shear-Stress Transport (SST) k-ω Turbulence Model:

$$\frac{\partial(\rho \mathrm{k})}{\partial t} + \nabla\cdot(\rho \mathrm{k} u) = \nabla\cdot(\Gamma_k \nabla\cdot k + G_k - Y_k + S_k) \tag{4}$$

$$\frac{\partial(\rho\omega)}{\partial t} + \nabla\cdot(\rho\omega u) = \nabla\cdot(\Gamma_\omega \nabla\cdot\omega + G_\omega - Y_\omega + D_\omega + S_\omega) \tag{5}$$

where:

u—velocity vector, m/s;
k—turbulent kinetic energy;
ε—turbulent kinetic energy dissipation rate;
ω—specific dissipation rate
Γ, Γ_k, Γ_ω—effective diffusivity for velocity (u), turbulent kinetic energy (k), and specific dissipation rate (ω)
G_k, G_ω—Production Terms for Turbulent Kinetic Energy (k) and Specific Dissipation Rate (ω)
Y_k, Y_ω—Dissipation Terms for Turbulent Kinetic Energy (k) and Specific Dissipation Rate (ω)
D_ω—Cross-Diffusion Term
S_k, S_ω—User-Defined Source Terms

(5) Species Transport Model:

$$\frac{\partial(\rho_i \alpha_i)}{\partial t} + \nabla\cdot(u\rho_i\alpha_i) = S_i \tag{6}$$

where:

α_i—mass fraction of species i, %;
ρ_i—density of the mixture, kg/m^3;
u—velocity vector, m/s;
S_i—source term for species i.

3. Numerical Simulation Setup

3.1. Physical Geometry Model Construction

To accurately represent the actual environment of a typical confined kitchen space, this study established a full-scale, proportional physical model (Figure 1). The spatial dimensions of the model were set to a length of 4 m, a width of 3 m, and a height of 2.8 m. Based on a typical kitchen layout, key components inside the model were detailed, including the gas pipeline, stove counter, window, and door. The specific geometric dimension parameters for each entity are detailed in Tables 1 and 2. This modeling strategy aims to ensure that the geometric boundary conditions of the numerical simulation accurately characterize the spatial constraints and flow characteristics of the real-world scenario.

Based on the statistical analysis of historical gas leakage accidents and to investigate the impact of different leakage mechanisms on dispersion behavior, this study selected two typical types of leakage from the hose in front of the stove for numerical simulation. The specific scenarios for hydrogen-blended natural gas leakage are set as follows:

Chronic Degradation Leakage: This scenario simulates a sustained leakage caused by minor cracks in the main gas branch pipe due to factors such as pipeline corrosion and material aging.

Acute Penetration Leakage: This scenario simulates a sudden leakage resulting from a small hole formed in the gas connecting rubber hose due to external impact or puncture by hard objects.

The setup of these scenarios aims to characterize the progressive potential hazards and sudden failure modes, respectively, that may occur in actual kitchen environments. This approach enables a systematic investigation into the effects of different leakage causes on the release and accumulation processes of hydrogen-blended natural gas. The detailed parameter settings for the two leakage types are summarized in Table 3.

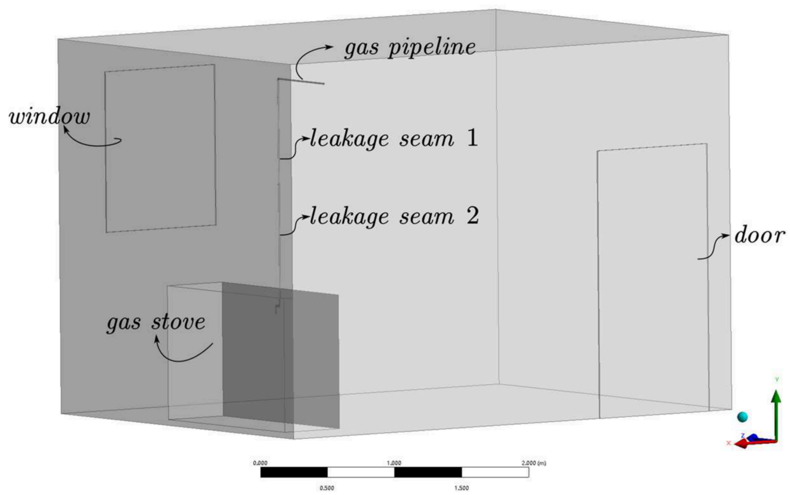

Figure 1. Physical Model of the Confined Space (outlet located at the bottom of the door).

Table 1. Specific Parameters for Geometric Model Construction.

Spatial Configuration	Exterior Wall (cm)	Window (cm)	Kitchen Counter (cm)	Door (cm)
Length	400	120	150	100
Width	300	100	50	5
Height Above Floor Level	280	130	120	200

Table 2. Gas Pipe Configuration Parameters.

Internal Diameter (mm)	External Diameter (mm)	Wall Thickness (mm)	Inlet Pressure (Pa)	Sheath Material
9.5	15.1	2.8	2500	Flame-Retardant PVC

Table 3. Parameter Settings for the Two Types of Hydrogen-Blended Natural Gas Leakage.

Leakage Source Type	Model Configuration	Leakage Area/mm^2
Crack leakage from the main rubber gas hose due to corrosion and other factors	Configured as a 5 cm long slit source (2 locations)	131.8
Pinhole leakage from the rubber gas hose caused by puncture from a hard object	Configured as a 4 mm diameter orifice source (3 locations)	37.7

3.2. Mesh Generation

Following the completion of the physical model, an unstructured mesh was generated using the Ansys Meshing module (ANSYS, Inc., Canonsburg, PA, USA) module. The global computational domain was discretized using tetrahedral elements, with a base element size set to 100 mm.

Considering the significant scale difference between the overall confined space and key components such as the gas pipeline, local mesh refinement was applied to the pipeline region to balance computational accuracy and efficiency, with its element size controlled to 1 mm. To further accurately capture the gradients in the flow field and volume fraction field near the leakage source, the "Body of Influence" (BOI) technique was employed to implement refined mesh control around the pipeline and leakage area, with the refinement size also set to 1 mm.

Through the aforementioned multi-level meshing strategy, the final computational mesh consisted of between 7,000,000 and 8,000,000 elements. To verify the independence of the calculation results from the mesh density, a grid independence study was conducted. A systematic grid independence study was conducted using four different mesh sizes: 0.2 m, 0.1 m, 0.05 m, and 0.02 m. The concentration of CH_4 at monitoring point P1 (located above the cooker at 1.2 m height) at t = 500 s was recorded for each grid. The results showed that the concentration changed from 2.01 vol% (0.2 m) to 2.10 vol% (0.1 m) to 2.17 vol% (0.05 m) and to 2.19 vol% (0.02 m). As the grid refines from 0.05 m to 0.02 m, the concentration changes by less than 1%, indicating that the 0.05 m grid (approximately 7.5 million cells) provides sufficient resolution for grid-independent results. The time-history curves of gas volume fraction at key monitoring points and the velocity distribution of the flow field were also compared. As shown in Table 4, the results further confirmed that the relative deviation between the medium (0.05 m) and fine (0.02 m) meshes was less than 3%, and the main flow characteristics remained consistent. Balancing computational accuracy and efficiency, the medium-density mesh (0.05 m, approximately 7.5 million cells) was ultimately selected for all numerical simulations. The computational mesh of the confined space is shown in Figure 2.

Table 4. Grid Independence Study Results (Concentration at Monitoring Point P1 at t = 500 s).

Grid Size	Cell Count (Approx.)	CH_4 Volume Fraction at P1 (vol%)	Deviation from 0.02 m
0.2 m	~0.5 million	2.01	7.8%
0.1 m	~2.0 million	2.10	3.7%
0.05 m	~7.5 million	2.17	0.9%
0.02 m	~12.0 million	2.19	—

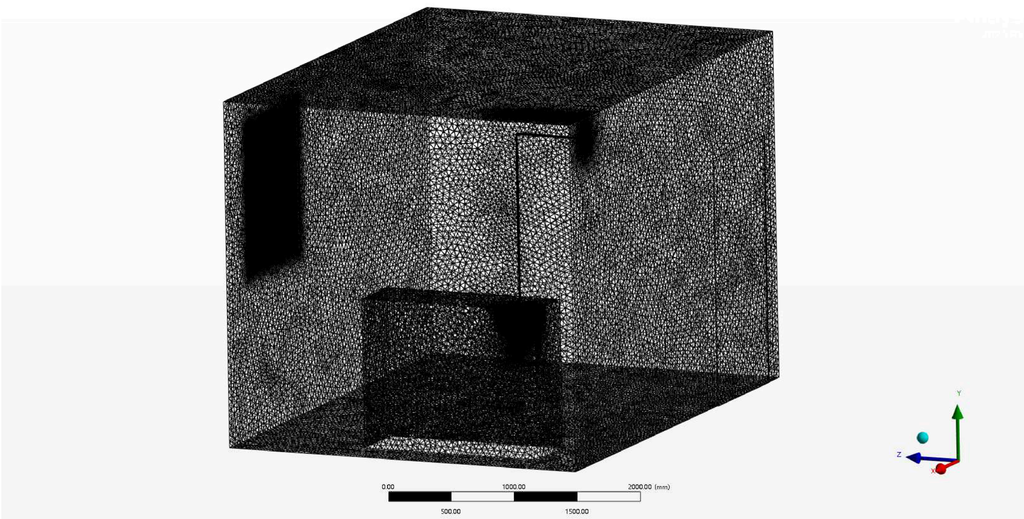

Figure 2. Computational Mesh.

3.3. Parameter Settings for FLUENT Numerical Calculation

To accurately simulate the actual leakage scenario, the key computational parameters in this study were set as follows: Hydrogen-blended natural gas was simplified as a binary mixture composed of methane and hydrogen. Comparative studies were conducted using three hydrogen blending ratios: 0% (pure methane), 10%, and 20% (by volume). Based on prior verification, the influence of neglecting other trace components on the simulation accuracy was deemed negligible.

Numerical simulations of the transient leakage and dispersion process of hydrogen-blended natural gas within the confined space were performed using the ANSYS FLUENT software (version 2023 R1, ANSYS, Inc., Canonsburg, PA, USA). The study first systematically simulated the gas dispersion dynamics under different leakage rates when the space was completely sealed. Building upon this, the influence of external air convection on the transport, distribution, and dispersion mechanisms of the hydrogen-blended natural gas cloud was further investigated under conditions with window ventilation (semi-confined state).

Through the design of the aforementioned working conditions, this research aims to systematically reveal the spatiotemporal distribution patterns and risk characteristics of the flammable gas within the confined space under the coupled effects of multiple factors, including the hydrogen blending ratio, spatial ventilation conditions, and leakage rate. The key computational parameters for the leakage and dispersion simulations are summarized in Table 5.

Table 5. Parameter Settings for Hydrogen-Blended Natural Gas Leakage in a Confined Space.

Item	Parameter Setting
Solver Type	Pressure-Based
Solver Time	Transient
Model	SST $k - \omega$ and Species Transport
Material	Methane-Hydrogen-Air
Operating Pressure	101,325 Pa (absolute)
Operating Temperature	288.16 K
Leakage Inlet Boundary	Velocity Inlet (velocity calculated from leak area and mass flow rate)
Window Boundary (Ventilation)	Velocity Inlet (uniform, 1.0 m/s, direction normal to window plane)
Outlet Boundary (Door Gap)	Pressure Outlet (0 Pa gauge)
Walls	No-slip Wall, adiabatic
Time Step Size	0.01 s
Total Simulated Time	1500 s
Convergence Criteria	Residuals $< 1 \times 10^{-4}$
Pressure-Velocity Coupling	SIMPLE
Spatial Discretization	Second-Order Upwind

For the open-window (semi-confined) scenarios, the window is modeled as a uniform velocity inlet with a constant wind speed of 1.0 m/s, representing a typical gentle breeze under natural ventilation conditions. This simplified boundary condition is adopted to focus on the fundamental effects of ventilation on gas dispersion, while acknowledging that realistic wind profiles may be more complex. The outlet is defined as the door gap (0.01 m height at the bottom of the door), which is set as a pressure outlet at 0 Pa gauge.

4. Simulation Results and Analysis

4.1. Natural Gas Leakage Dispersion Trajectories

To systematically investigate the dispersion characteristics of hydrogen-blended natural gas under different leakage conditions, this study conducted comprehensive numerical simulations of the transient dispersion processes for two types of leakage orifices (crack leakage and small hole leakage) within the confined space across all working conditions. Through comparative analysis of scenarios with different hydrogen blending ratios (0%, 10%, 20%), the time-varying volume fraction fields and velocity fields of the combustible gas within the space were obtained. Furthermore, key dynamic parameters such as the maximum jet velocity, vortex scale, and gas displacement efficiency were quantified. Figure 3 illustrates the particle trajectories of hydrogen-blended natural gas during leakage and dispersion.

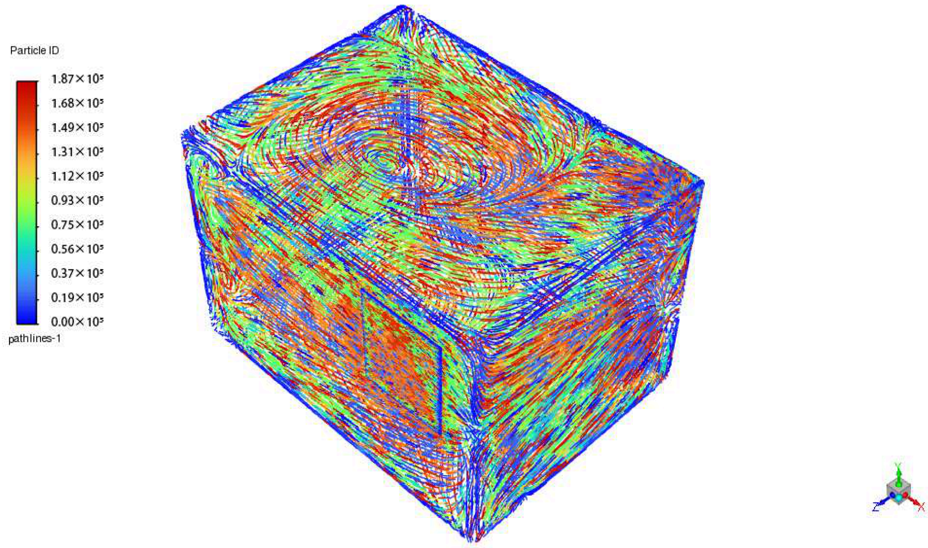

Figure 3. Particle Trajectories of Hydrogen-Blended Natural Gas during Leakage and Dispersion.

To intuitively reveal the transport pathways and spatial distribution patterns of the leaked gas, the CFD-POST professional post-processing tool was employed for the visualization of Fluent calculation results. By extracting and plotting gas dispersion trajectory diagrams at characteristic time points, the dynamic entire process—from initial jetting, through spatial migration, to final accumulation—of the natural gas cloud under different leakage scenarios was clearly demonstrated. This visualization method not only effectively reveals the influence of both the leakage source characteristics and the hydrogen blending ratio on the dispersion patterns but also provides an intuitive basis for the quantitative analysis of the evolution of combustible regions.

Figure 4 displays the particle dispersion trajectories of hydrogen-blended natural gas from a crack leakage in the main gas pipe. The simulation results indicate that after release from the leakage source, the gas exhibits a distinct vortex-like dispersion pattern and accumulates along the wall surfaces. Due to the significantly lower density of hydrogen-blended natural gas compared to air, the leaked gas primarily moves upward under buoyancy, eventually accumulating at the top of the confined space. The initial jet velocity reaches up to 1.5 m/s but rapidly decays to below 0.25 m/s after impacting the ceiling. The fluid particles, after being ejected from the leakage source, undergo rotational motion within the space, experiencing complex processes such as mixing with air, collisions, and multiple wall reflections, ultimately forming a distribution characterized by vortex-dominated dispersion. It is crucial to emphasize that the vortex structures present in the turbulent flow have a decisive influence on gas mixing efficiency. Large-scale vortices are responsible for rapidly transporting the gas to distant areas of the space, while small-scale vortices enhance the diffusion from high-concentration to low-concentration regions through intense local mixing. This mechanism significantly affects the evolution speed of the combustible gas cloud and the extent of hazardous zone formation.

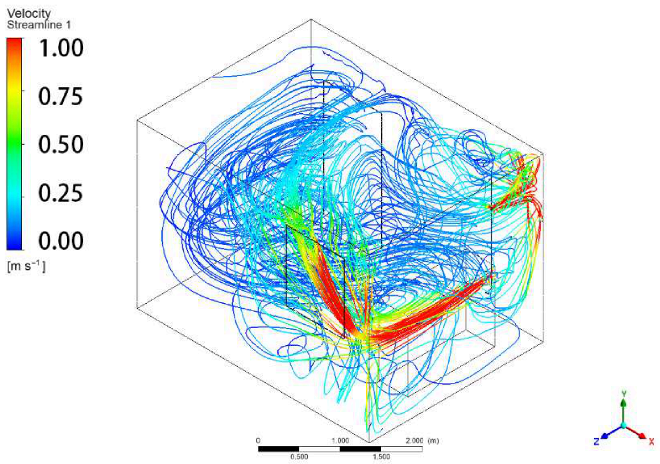

Figure 4. Gas Dispersion Pathlines from a Crack Leakage in the Main Gas Pipeline.

Figure 4 illustrates the velocity distribution of the flow field following a crack leakage in the main gas pipe. The simulation results indicate that during the initial leakage stage, the gas velocity exceeds 1.5 m/s, significantly influencing the flow field structure within the confined space. Driven by this high-speed jet, both the speed and direction of natural gas dispersion undergo continuous and marked changes, resulting in a highly transient and turbulent flow field. Dominated by the buoyancy effect due to the lower density of hydrogen-blended natural gas compared to air, the leaked gas primarily moves upward after release and forms a horizontal spread along the ceiling, constrained by the roof. The airflow velocity in this horizontal spreading region decreases to approximately 0.2 m/s but continues to generate velocity fluctuations and disturbances within the space. From the perspective of turbulent structure evolution, this leakage and dispersion process exhibits typical multi-scale vortex characteristics. The gas is initially entrained by large-scale vortices, causing gas clusters to rotate, stretch, and be rapidly transported over a larger spatial extent. Within this large-scale vortex framework, numerous small-scale vortex structures develop. These secondary vortices significantly enhance the turbulent dispersion rate and final mixing efficiency of the gas by intensifying local mixing.

Figure 5 illustrates the dispersion trajectory distribution under the condition of a small-orifice leakage of natural gas. The simulation results indicate that the dispersion pattern of the small-orifice leakage is primarily characterized by lateral spreading during the initial stage, with an initial jet velocity of approximately 0.8 m/s, which is lower than that of the crack leakage. When the jet interacts with the wall surface, the wall boundary significantly impedes the flow, causing a noticeable decay in airflow velocity after reflection, reducing it to about 0.25 m/s. When the flow path encounters obstacles or changes in spatial structure, several small-scale vortices form locally, but the overall flow structure maintains relatively regular dispersion trajectories. Comparative analysis with the crack leakage case shown in Figure 5 reveals significant differences in flow characteristics between the two: due to the larger leakage area in the crack leakage, the velocity in the jet core region is better maintained, and the influence of buoyancy is more pronounced, resulting in a more prominent upward transport trend. In contrast, for the small-orifice leakage, the restricted flow area leads to a relatively lower mass flow rate per unit time and smaller initial kinetic energy, consequently resulting in slower upward transport and overall dispersion rate.

Integrating the flow field characteristics of both leakage modes, it is observed that the velocity is highest near the leakage source and gradually decays with increasing dispersion distance. In the initial jet region, lateral dispersion dominates, with limited spatial expansion. As the flow develops downstream, turbulent mixing intensifies, and the gas dispersion range gradually expands, exhibiting typical evolution patterns of a confined jet.

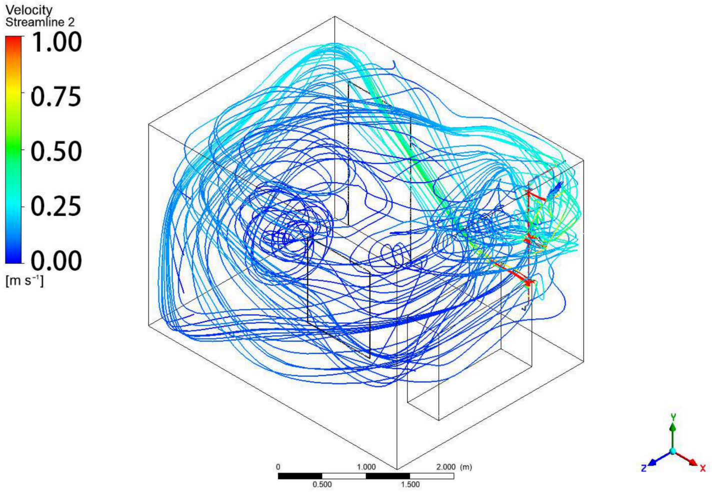

Figure 5. Gas Dispersion Pathlines from a Pinhole Leakage in the Rubber Gas Hose.

4.2. Dispersion and Distribution Patterns of Hydrogen-Blended Natural Gas Leakage

The lower flammability limit (LFL) of a fuel-air mixture is not constant when hydrogen is added. For pure methane, the LFL is 5.0 vol% under standard conditions. For hydrogen-methane mixtures, the LFL decreases slightly with increasing hydrogen content due to hydrogen's wider flammability range (LFL_{H2} = 4.0 vol%). To provide a rigorous basis for safety assessment, the mixture LFL for each hydrogen blending ratio was calculated using Le Chatelier's law:

$$LFL_{mix} = \frac{1}{y_{CH_4}/LFL_{CH_4} + y_{H_2}/LFL_{H_2}} \tag{7}$$

where LFL_{CH4} = 5.0 vol%, LFL_{H2} = 4.0 vol%, and y_{CH4} and y_{H2} are the volume fractions of methane and hydrogen in the fuel mixture (i.e., excluding air). This yields mixture LFLs of 5.00 vol% (0% H_2), 4.88 vol% (10% H_2), and 4.76 vol% (20% H_2). Using these mixture-specific LFLs instead of a fixed 5% threshold would reduce the reported time to reach LFL by approximately 3–5%, which does not alter the overall conclusions of this study.

For consistency in visualizing the contour plots across all blending ratios, and to facilitate intuitive identification of hazardous zones, the color scale upper limit in Figures 6–14 is uniformly set to 5 vol%. This value approximates the LFL of all mixtures investigated (deviations $\leq$ 0.24 vol%). Accordingly, deep red areas in the figures indicate regions where the total fuel (CH_4 + H_2) volume fraction is approximately at or above the flammable threshold.

This visualization method not only enables intuitive comparison of gas dispersion paths and accumulation characteristics across different leakage scenarios but also provides an effective basis for quantitatively analyzing the formation time, spatial extent, and duration of flammable clouds, thereby supporting subsequent safety assessments and risk analysis.

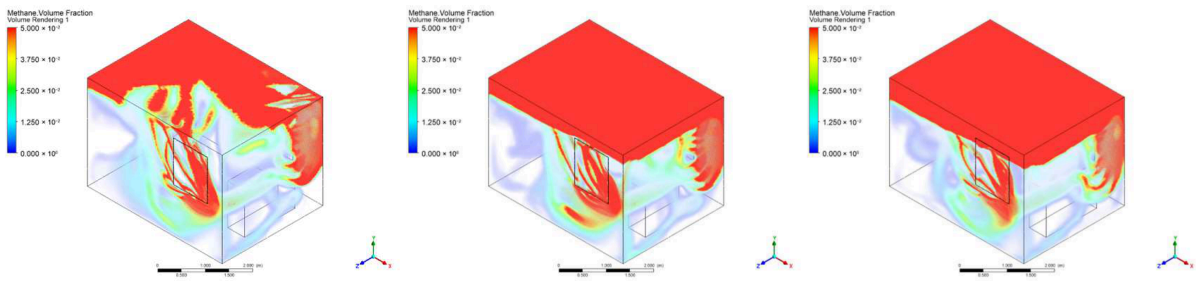

1 min 10 min 25 min

Figure 6. Volume fraction distribution (total fuel: CH_4 + H_2) for the crack leakage scenario in a confined space (no ventilation) with 0% H_2 blending ratio, shown at t = 1 min, 10 min, and 25 min.

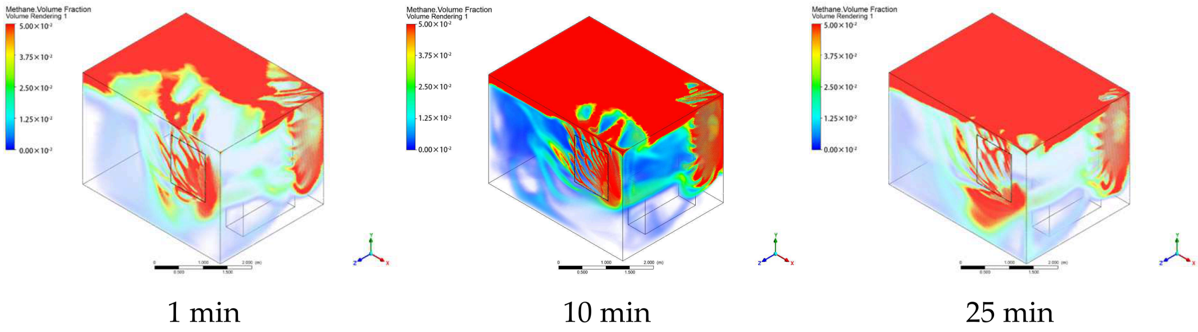

Figure 7. Volume fraction distribution (total fuel: CH_4 + H_2) for the crack leakage scenario in a confined space (no ventilation) with 10% H_2 blending ratio, shown at t = 1 min, 10 min, and 25 min.

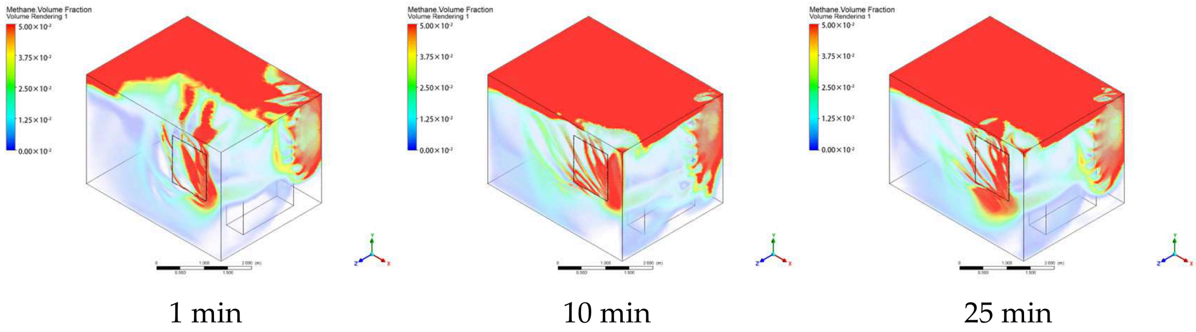

Figure 8. Volume fraction distribution (total fuel: CH_4 + H_2) for the crack leakage scenario in a confined space (no ventilation) with 20% H_2 blending ratio, shown at t = 1 min, 10 min, and 25 min.

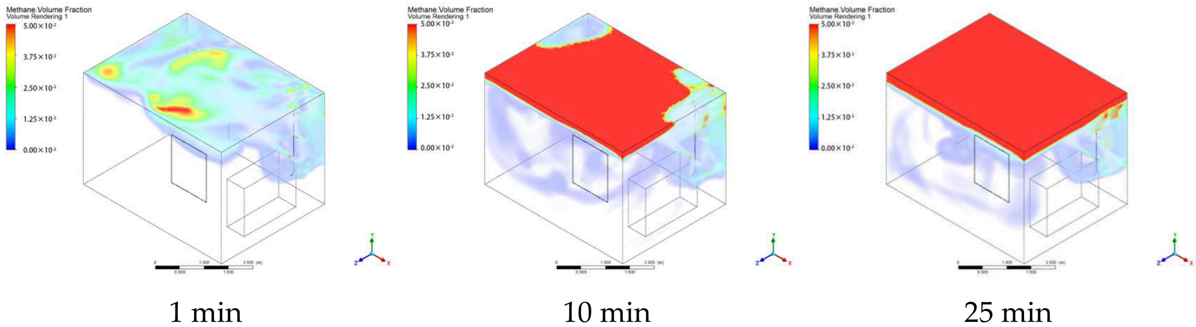

Figure 9. Volume fraction distribution (total fuel: CH_4 + H_2) for the pinhole leakage scenario in a confined space (no ventilation) with 0% H_2 blending ratio, shown at t = 1 min, 10 min, and 25 min.

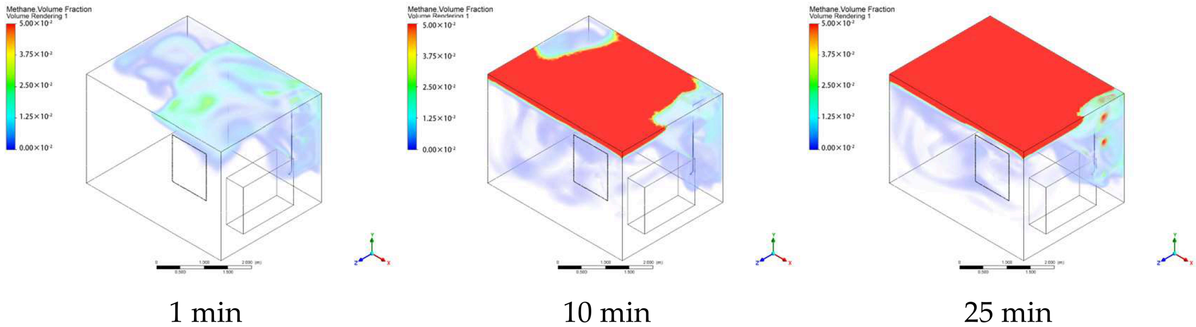

Figure 10. Volume fraction distribution (total fuel: CH_4 + H_2) for the pinhole leakage scenario in a confined space (no ventilation) with 10% H_2 blending ratio, shown at t = 1 min, 10 min, and 25 min.

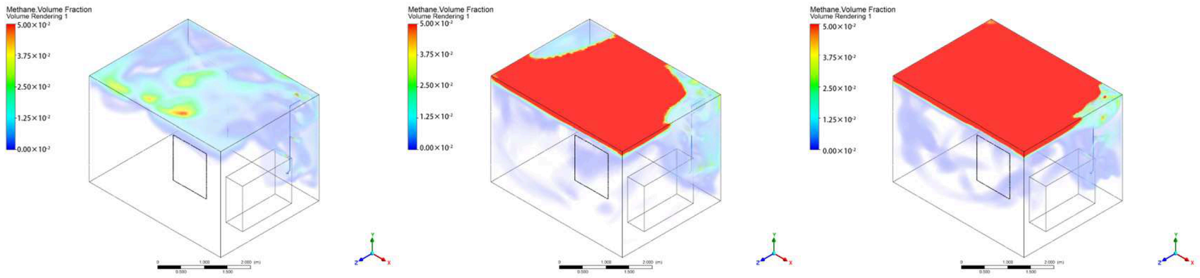

1 min 10 min 25 min

Figure 11. Volume fraction distribution (total fuel: $CH_4 + H_2$) for the pinhole leakage scenario in a confined space (no ventilation) with 20% H_2 blending ratio, shown at t = 1 min, 10 min, and 25 min.

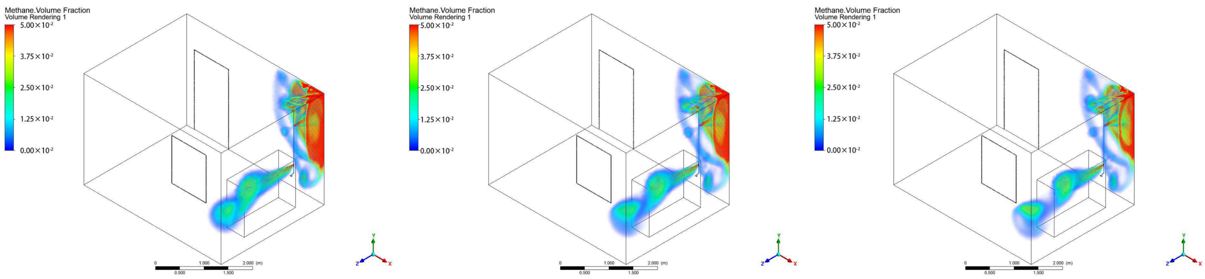

1 min 10 min 25 min

Figure 12. Volume fraction distribution (total fuel: $CH_4 + H_2$) for the crack leakage scenario in an open space (window ventilation) with 0%, 10%, and 20% H_2 blending ratios, shown at t = 1 min, 10 min, and 25 min.

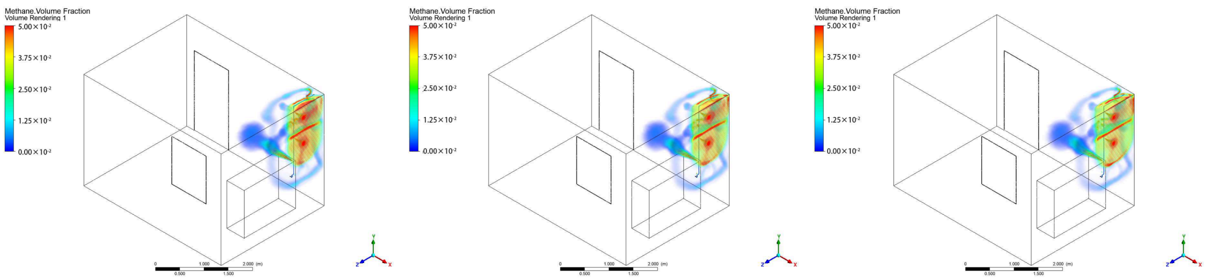

1 min 10 min 25 min

Figure 13. Volume fraction distribution (total fuel: $CH_4 + H_2$) for the pinhole leakage scenario in an open space (window ventilation) with 0%, 10%, and 20% H_2 blending ratios, shown at t = 1 min, 10 min, and 25 min.

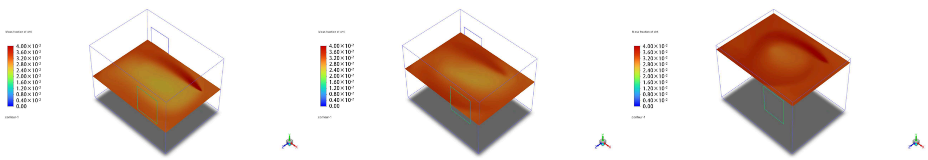

at the stove level (height = 1.2 m) | at the specified level (height = 1.6 m) | at the ceiling light level (height = 2.6 m)

Figure 14. Gas volume fraction distribution at 500 s for pinhole leakage in a confined space.

4.2.1. Confined Space: No Wind Inflow

Figure 6 illustrates the spatiotemporal evolution of the gas volume fraction distribution within the confined space for a crack leakage scenario caused by factors such as corrosion.

The simulation results indicate that during the initial stage following leakage (within 1 min), the gas rapidly forms a jet primarily moving vertically after escaping from the crack, while also spreading laterally during its ascent. At this point, localized areas near the top of the space already exhibit gas volume fractions exceeding 5%, i.e., regions that have reached the LFL.

Due to the high initial momentum and lateral dispersion capability characteristic of the crack leakage mode, after 15 min, the hydrogen-blended natural gas has spread and accumulated across the entire ceiling area, forming a high-volume-fraction gas accumulation layer with a thickness exceeding 0.2 m. In the vicinity of the leakage source near the wall and the window, the gas volume fraction reaches or exceeds the LFL, indicating a high local risk of combustion and explosion. By 25 min post-leakage, natural gas with different hydrogen blending ratios exhibits typical stratified distribution characteristics. Pure methane (0% hydrogen blending ratio) forms a high-concentration accumulation layer approximately 0.4 m thick in the upper part of the space, presenting a clear vertical stratification structure within the space. In contrast, for gas mixtures with 10% and 20% hydrogen blending ratios, influenced by the strong diffusivity and buoyancy of hydrogen, the resulting upper accumulation layer is thinner, about 0.3 m, but still demonstrates a similar stratified distribution trend.

To quantify the risk, the temporal evolution of the flammable cloud volume (regions where the total fuel volume fraction exceeds the mixture-specific LFL: 5.00% for 0% H_2, 4.88% for 10% H_2, and 4.76% for 20% H_2) was analyzed, as shown in Figure 7. It can be observed that the growth of the gas cloud volume for all scenarios exhibits a three-phase characteristic: "slow accumulation—rapid increase—trend towards saturation". An increase in the hydrogen blending ratio significantly shortens the time for the gas cloud volume to enter the rapid growth phase. For instance, for the scenario with 20% hydrogen blending, the gas cloud volume begins its explosive growth around 400 s after leakage, nearly 100 s earlier than the pure methane scenario, and reaches approximately 8.5 m^3 by about 600 s, accounting for over 25% of the total space volume. Table 6 presents the time to reach the mixture-specific LFL at each monitoring point for the crack leakage scenario.

Table 6. Time to reach the mixture-specific lower flammability limit (LFL) for the crack leakage scenario (unit: s).

Monitoring Point Location	H_2 Vol 0%	H_2 Vol 10%	H_2 Vol 20%
Above the Cooker (P1)	580	520	450
Middle of the Space (P2)	720	650	570
Near the Ceiling Light (P3)	480	420	380

Note: The times reported in Table 6 were calculated using a 5% threshold for consistency with the contour plot visualization. Since the mixture-specific LFLs for 10% H_2 and 20% H_2 are 4.88% and 4.76%, respectively, using these more precise values would reduce the reported times by approximately 3–5%. This minor adjustment does not affect the comparative trends or the main conclusions of this study.

Based on the comparative analysis of Figures 6–9, it is observed that while the spatiotemporal evolution trends of the volume fraction for hydrogen-blended natural gas with different hydrogen blending ratios are generally consistent during the leakage and dispersion process, the key dispersion parameters are significantly influenced by the hydrogen blending ratio. As the hydrogen blending ratio increases, the dispersion capacity of the methane component in the mixture relatively weakens, manifested as a gradual reduction in the dispersion range of methane within the same time frame. Concurrently, due to its low molecular weight and high diffusion coefficient, the hydrogen component experiences a significant expansion in both its horizontal and vertical dispersion ranges. This coupling effect results in the following characteristics for the overall dispersion behavior of hydrogen-blended natural gas: although the time required for the leaked gas to reach the top boundary of the model shows a slow decreasing trend with increasing hydrogen blending ratio, both the vertical migration distance and the dispersion rate of the gas are significantly enhanced, reflecting the strengthening effect of hydrogen on the buoyancy and dispersion dynamics of the gas mixture.

The aforementioned results indicate that an increase in the hydrogen blending ratio alters the compositional structure and physical properties of the leaked gas. This, in turn, affects the distribution pattern and accumulation characteristics of the flammable gas within the space by modulating its buoyancy characteristics and turbulent dispersion process.

Figures 9–11 illustrate the dynamic distribution of gas volume fraction within the confined space under a scenario involving a small-hole leakage in the gas rubber hose caused by puncture from a hard object. The simulation results indicate that within 1 min of leakage initiation, two localized gas accumulation zones, where the volume fraction reaches the lower flammability limit of natural gas, have already appeared near the top of the space. Compared to the crack leakage, the small-hole leakage exhibits a relatively slower initial dispersion velocity due to its smaller leakage flux. By 15 min post-leakage, the hydrogen-blended natural gas forms a large-area accumulation at the ceiling, with an accumulation layer thickness exceeding 0.1 m, and the gas volume fraction in the leakage source vicinity and adjacent wall regions exceeds the lower flammability limit. After 25 min of leakage, a stable, high-concentration accumulation layer approximately 0.3 m thick forms in the upper part of the space. Quantitative analysis of the flammable cloud volume for the small-hole leakage scenario reveals a growth pattern similar to that of the crack leakage, but the overall process is delayed. Table 7 gives the corresponding results for the pinhole leakage scenario.

Table 7. Time to reach the mixture-specific lower flammability limit (LFL) for the pinhole leakage scenario (unit: s).

Monitoring Point Location	H_2 Vol 0%	H_2 Vol 10%	H_2 Vol 20%
Above the Cooker (P1)	720	650	580
Middle of the Space (P2)	860	780	700
Near the Ceiling Light (P3)	620	550	550

Note: The times reported in Table 6 were calculated using a 5% threshold for consistency with the contour plot visualization. Since the mixture-specific LFLs for 10% H_2 and 20% H_2 are 4.88% and 4.76%, respectively, using these more precise values would reduce the reported times by approximately 3–5%. This minor adjustment does not affect the comparative trends or the main conclusions of this study.

It is noteworthy that in real kitchen environments, potential ignition sources such as the stove ignition zone and overhead lighting fixtures, which can readily produce open flames or electrical sparks, are present. The simulation results reveal that the locations of these ignition sources exhibit a high degree of spatial overlap with the high-concentration gas accumulation zones. This creates a coupled "hazard zone-ignition source" scenario, which significantly increases the probability of leaked gas being ignited and consequently exacerbates both the explosion risk and the potential severity of accidents resulting from indoor natural gas leakage.

4.2.2. Open Space: Natural Wind Inflow Through Window

To investigate the impact of an open computational domain on the leakage and dispersion behavior of hydrogen-blended natural gas, the window in the physical model was set to an open state, transforming the originally sealed space into an open space connected to the atmosphere. Under these conditions, the external wind field becomes a critical factor influencing gas dispersion. To accurately simulate the actual ventilation environment, the open-window boundary was modeled as a uniform velocity inlet with a constant wind speed of 1.0 m/s, as described in Section 3.3. This enabled the precise simulation of the quasi-steady-state dissipation process of hydrogen-blended natural gas leakage and dispersion under natural ventilation in an open space.

(1) Analysis of Main Gas Pipe Crack Leakage Scenario

Figure 13 displays the dispersion situation resulting from a crack leakage in the main gas pipe, caused by factors such as corrosion, under open-window conditions. The simulation results indicate that the incoming airflow through the window significantly influences the dispersion behavior of the crack leakage. Unlike the scenario where the sealed space becomes filled with a gas cloud, the risk characteristic in the open-window scenario shifts to "localized high concentration." A small area of high volume fraction forms near the leakage source, with a concentration significantly higher than in other parts of the space. Although the incoming air through the window accelerates the overall dissipation process of the hydrogen-blended natural gas, gas accumulation and local aggregation still occur near the leakage source. It is particularly noteworthy that the natural gas volume fraction in a small area near the leakage source reaches 5%, exceeding the lower flammability limit and creating a localized explosion hazard zone.

Notably, while window ventilation promotes global dispersion, it can also lead to the formation of a stable, high-concentration gas cloud in the immediate vicinity of the leakage source. Monitoring revealed that within 0.5 m downstream of the leakage source, the volume fraction stabilized between 5% and 8% within 200 s after the leak started, forming a "persistent hazardous zone" that highly overlaps with ignition sources such as stoves. This "risk transfer" phenomenon indicates that ventilation alone cannot completely eliminate the risk of combustion and explosion, making rapid shutoff of the leakage source and concentration monitoring in the near-source area crucial.

The leakage and dispersion trends of natural gas with different hydrogen blending ratios under open-window conditions are generally consistent. As the hydrogen blending ratio increases, the dispersion range of the methane component in the mixture relatively shrinks, manifested as a gradual decrease in the leakage dispersion volume fraction. In contrast, the hydrogen component, leveraging its higher dispersion capacity and volatility, significantly expands its dispersion range in both horizontal and vertical directions. Benefiting from hydrogen's tendency to mix rapidly with air, the likelihood of hydrogen-blended natural gas accumulating on walls and within the space is relatively reduced. However, the characteristic local high risk near the leakage source still requires sufficient attention.

(2) Small-hole Leakage in Gas Rubber Hose Caused by Hard Object Puncture

Figure 14 illustrates the dispersion situation under open-window conditions for a small-hole leakage in the gas rubber hose caused by hard object puncture. The simulation results indicate that the airflow generated by the incoming wind through the window significantly influences the leakage and dispersion behavior of the hydrogen-blended natural gas. The maximum incoming wind speed at the window reaches 2 m/s, effectively promoting the transport and dissipation of the leaked gas. However, similar to the crack leakage, ventilation also fails to completely eliminate the local high risk near the small-hole leakage source. Comparing the gas distribution under quasi-steady-state conditions for crack leakage (Figure 12) and small-hole leakage (Figure 13) reveals that a localized explosion hazard zone, where the volume fraction exceeds 5% (the lower flammability limit), also forms near the small-hole leakage source. also forms near the small-hole leakage source. As the hydrogen blending ratio increases, the dispersion range of hydrogen expands in both horizontal and vertical directions, while the dispersion range of methane correspondingly shrinks.

However, significant differences in spatial distribution characteristics exist between the two leakage types: the high-volume-fraction zone formed by small-hole leakage is smaller and closer to the leakage source. Due to the relatively lower leakage momentum, the gas stream mixes more readily with the ambient air and dilutes faster, but the resulting stable high-concentration gas cloud persists for a longer duration. In contrast, crack leakage, due to the better-maintained gas velocity, exhibits a relatively slower dispersion process and is more prone to forming stable accumulated gas clouds on walls and in localized areas, leading to persistent high-risk zones. This finding emphasizes that for small-hole leakage, even under ventilated conditions, areas close to the leakage source (such as beneath the stove) remain the critical focus for risk monitoring and prevention.

4.3. Multi-Factor Coupling Effects and Parameter Sensitivity Discussion

This study further comprehensively analyzes the coupling effects of multiple factors, including hydrogen blending ratio, leakage type, and ventilation conditions. By comparing metrics such as "flammable cloud volume" and "time to reach the lower flammability limit" across different working conditions, the following findings were obtained:

The hydrogen blending ratio is the most sensitive parameter affecting the dispersion rate and risk formation time. Increasing the hydrogen blending ratio expands the dispersion range of the hydrogen component but, under certain conditions, can enhance the near-source accumulation effect of methane.

The leakage type primarily influences the initial jet kinetic energy and the morphology of the hazardous zone. Crack leakage tends to form large-area, uniformly thick ceiling stratification, whereas small-hole leakage more easily forms localized high-concentration zones downstream of complex structures.

The ventilation condition determines whether the risk is global or local. In confined spaces, the risk is global (space filling), whereas in open spaces, the risk is local (near-source accumulation). The latter scenario demands heightened vigilance due to its concealed nature.

These findings provide a clear basis for formulating differentiated safety monitoring strategies. For instance, for scenarios with high hydrogen blending ratios or in open spaces, alarm installation should focus more on areas near the leakage source.

4.4. Experimental Validation

To effectively verify the accuracy of the numerical model established in this paper and the Fluent simulation results, a systematic comparative analysis between the simulation data and experimental results was conducted [15]. The experiment utilized an LB-MD4X fixed methane volume fraction intelligent detector to measure the natural gas volume fraction distribution within a confined space under the condition of a small-hole leakage in the gas rubber hose caused by hard object puncture. Measurement points were arranged based on characteristic spatial locations, selecting three representative positions: 1.2 m above the gas stove, at 1.6 m height in the middle of the space, and near the ceiling light at 2.6 m height. The measurement time was uniformly set at 500 s after leakage, representing a quasi-steady state.

A comparative analysis was performed between the volume fraction values measured at these three points in the experiment from reference [16] and the simulation results from the corresponding scenario in this study (Figure 14). The results show good agreement between the simulated and experimental values in both trend and magnitude. According to the quantitative comparison results listed in Table 8, the absolute deviations are within 0.9 percentage points, and the relative errors are 16.2%, 15.3%, and 9.2%, respectively. This validates the applicability and accuracy of the SST turbulence model, boundary condition settings, and meshing strategy adopted in this paper for simulating small-hole leakage scenarios in confined spaces. Table 8 compares the simulated volume fractions with the experimental measurements at the three monitoring points.

Table 8. Comparison of Measured and Simulated Natural Gas Volume Fractions.

Measurement Location	Experimental Value/%	Simulated Value/%	Absolute Error (Percentage Point)	Relative Error/%
Above Cooker (1.2 m Height)	1.85	2.15	0.3	16.2
Mid-Space (1.6 m Height)/	2.03	2.34	0.31	15.3
Near Ceiling Light/%	9.72	8.83	0.89	9.2

The comparison with experimental data shows that the numerical model can reasonably capture the concentration trends and spatial distribution of leaked gas, with absolute deviations within 0.9 percentage points and relative deviations within 16.2%. This provides confidence in using the model for parametric studies, although further validation with more detailed experimental data (including velocity fields and H_2 concentrations) would be beneficial.

5. Conclusions

This study systematically investigated the leakage and dispersion behavior of hydrogen-blended natural gas in indoor confined spaces using numerical simulation methods, focusing on the effects of hydrogen blending ratio, leakage type, and spatial openness on the dispersion characteristics and accident evolution patterns. The main conclusions are as follows:

(1) The hydrogen blending ratio significantly influences the leakage and dispersion behavior. The temporal variation trend of the volume fraction for natural gas with different hydrogen blending ratios is generally consistent after leakage. However, as the hydrogen blending ratio increases, the dispersion range of the methane component gradually shrinks, while hydrogen, leveraging its lower molecular weight and higher diffusion capacity, significantly expands its dispersion range in both horizontal and vertical directions. The time required for the leaked gas to reach the upper boundary of the model shows a slow decreasing trend with increasing hydrogen blending ratio, while the vertical migration distance increases noticeably.

(2) The leakage dynamic behavior exhibits typical jet and vortex coupling characteristics. The initial leakage velocity of hydrogen-blended natural gas exceeds 1 m/s. Under buoyancy, it moves upward to the upper part of the space, forming horizontal spread after reaching the ceiling, with the velocity dropping below 0.2 m/s. Multi-scale vortex structures form during the dispersion process. These vortices not only enhance the gas transport capacity in both horizontal and vertical directions but also promote rapid mixing from high-concentration to low-concentration zones. Both crack leakage and small-hole leakage exhibit significant lateral jet dispersion. Among them, crack leakage has a higher lateral velocity (greater than 1 m/s) and a longer sustained distance; the velocity gradually decays under the influence of gravity and air resistance, the jet cross-section expands, and a certain upward trend is observed.

(3) The leakage risk distribution is controlled by spatial confinement. In a confined space, a high-volume-fraction premixed layer with a thickness exceeding 0.3 m forms in the upper part after 25 min of leakage, with its volume fraction exceeding the lower flammability limit of methane. Under open-window ventilation conditions, localized high-concentration zones (volume fraction exceeding 5%) appear near the leakage source. Due to the spatial overlap of potential ignition sources (such as stove ignition zones and ceiling lights) with these high-concentration zones, a coupled "hazard zone-ignition source" scenario is formed, significantly increasing the combustion and explosion risk of the leaked gas.

It should be noted that the present validation is limited to point-wise concentration data for a single leakage scenario. Further experimental validation with velocity field measurements and hydrogen concentration data under varying ventilation conditions would strengthen the quantitative reliability of the model.

Author Contributions: Conceptualization, N.X.; Methodology, N.X. and R.Y.; Software, Z.Y.; Validation, Z.Y.; Formal analysis, Z.Y.; Investigation, Z.Y. and Q.S.; Data curation, N.X., Q.S. and R.Y.; Visualization, L.W.; Supervision, L.W. All authors have read and agreed to the published version of the manuscript.

Funding: This research was funded by Guangdong University of Petrochemical Technology grant number 2023bsqd1014, and the Maoming Science and Technology Program grant numbers 240516164559939 and 240520164550381. The APC was funded by Guangdong University of Petrochemical Technology.

Data Availability Statement: The original contributions presented in this study are included in the article. Further inquiries can be directed to the corresponding author.

Conflicts of Interest: The authors declare no conflicts of interest.

References

1. Li, J.; Yu, B.; Su, Y.; Liu, C.; Li, Y. Concentration distribution of hydrogen-blended natural gas under static conditions. *Nat. Gas. Ind.* **2024**, *44*, 145–155.
2. Lagioia, G.; Spinelli, M.P.; Amicarelli, V. Blue and green hydrogen energy to meet European Union decarbonisation objectives. An overview of perspectives and the current state of affairs. *Int. J. Hydrogen Energy* **2023**, *48*, 1304–1322. [CrossRef]
3. Liu, B.; Liu, S.; Guo, S.; Zhang, S. Economic study of a large-scale renewable hydrogen application utilizing surplus renewable energy and natural gas pipeline transportation in China. *Int. J. Hydrogen Energy* **2019**, *45*, 1385–1398. [CrossRef]
4. Erdener, B.C.; Sergi, B.; Guerra, O.J.; Chueca, A.L.; Pambour, K.; Brancucci, C.; Hodge, B.-M. A review of technical and regulatory limits for hydrogen blending in natural gas pipelines. *Int. J. Hydrogen Energy* **2023**, *48*, 5595–5617. [CrossRef]
5. Pluvinage, G.; Capelle, J.; Hadj Meliani, M. Pipe networks transporting hydrogen pure or blended with natural gas, design and maintenance. *Eng. Fail. Anal.* **2019**, *106*, 104164. [CrossRef]
6. Pellegrini, M.; Guzzini, A.; Saccani, C. A Preliminary Assessment of the Potential of Low Percentage Green Hydrogen Blending in the Italian Natural Gas Network. *Energies* **2020**, *13*, 5570. [CrossRef]
7. Lynch, F.E.; Marmaro, R.W. Special Purpose Blends of Hydrogen and Natural Gas. U.S. Patent Application US07/607; US05139002A, 27 June 2024.
8. Tlili, O.; Mansilla, C.; Frimat, D.; Perez, Y. Hydrogen market penetration feasibility assessment: Mobility and natural gas markets in the US, Europe, China and Japan. *Int. J. Hydrogen Energy* **2019**, *44*, 16048–16068. [CrossRef]
9. Chan, S.T. *Recent Upgrades and Enhancements of the FEM3A Model*; Office of Scientific Technical Information Technical Reports: Oak Ridge, TN, USA, 1994.
10. Kim, E.; Park, J.; Cho, J.H.; Moon, I. Simulation of hydrogen leak and explosion for the safety design of hydrogen fueling station in Korea. *Int. J. Hydrogen Energy* **2013**, *38*, 1737–1743. [CrossRef]
11. Haines, M.R.; Polman, E.A.; de Laat, J.C. *Reduction of CO_2 Emissions by Addition of Hydrogen to Natural Gas*; IEA Greenhouse Gas R&D Programme: Cheltenham, UK, 2004.
12. Wilkening, H.; Baraldi, D. CFD modelling of accidental hydrogen release from pipelines. *Int. J. Hydrogen Energy* **2007**, *32*, 2206–2215. [CrossRef]
13. Wang, X.; Xu, H.; Chen, D.; Zhao, Z.; Huang, Y.; Ren, S.; Duo, B. Study on the diffusion behavior of hydrogen-blended natural gas pipeline leakage under the influence of obstacles. *Chem. Saf. Environ.* **2023**, *36*, 12–21.
14. Su, Y.; Li, J.; Yu, B.; Zhao, Y. Numerical investigation on the leakage and diffusion characteristics of hydrogen-blended natural gas in a domestic kitchen. *Renew. Energy* **2022**, *189*, 899–916. [CrossRef]
15. Wang, J.; Duan, W.; Li, C.; Shi, L.; Ma, C.; Jing, Y. Numerical simulation of the diffusion process of natural gas leakage in a kitchen. *J. Saf. Environ.* **2022**, *22*, 298–305. [CrossRef]
16. Wang, J.; Li, C.; Duan, W.; Zhang, Q.; Shi, L.; Ma, C. Experimental study of indoor natural gas leakage process. *J. Saf. Environ.* **2022**, *22*, 292–297. [CrossRef]